

A Multiphysics Implicit-Explicit Time Integration Algorithm for Simulating Tokamak-Edge Plasma Dynamics

U.S. National Congress on Computational Mechanics
Albuquerque, New Mexico



July 2023

Debojyoti Ghosh, Mikhail Dorf, Milo Dorr, Lee Ricketson



Challenges in Simulating Tokamak-Edge Plasma Dynamics

Kinetic effects are essential

- Strong deviations from the Maxwellian distribution
- Large poloidal variation in the electrostatic potential

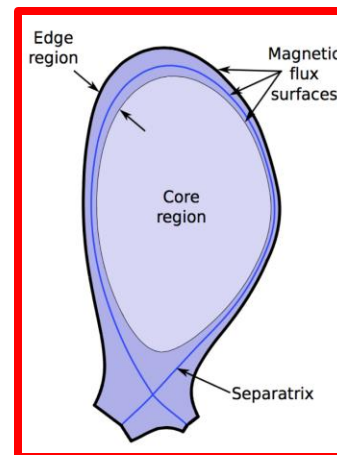
High-dimensionality of governing equations

Complicated geometry and anisotropy

- Magnetic separatrix and X-point
- Physical boundaries
- **Strong magnetic field** implies parallel advection much larger than perpendicular drifts

Collision regimes vary rapidly

- Weakly-collisional in the hot core
- Strongly-collisional in the cold edge



ITER tokamak

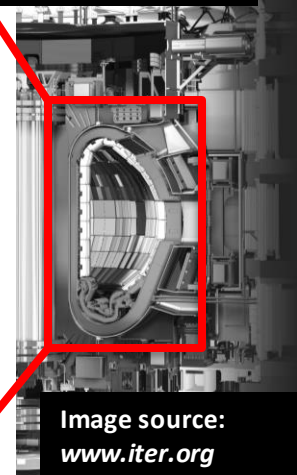
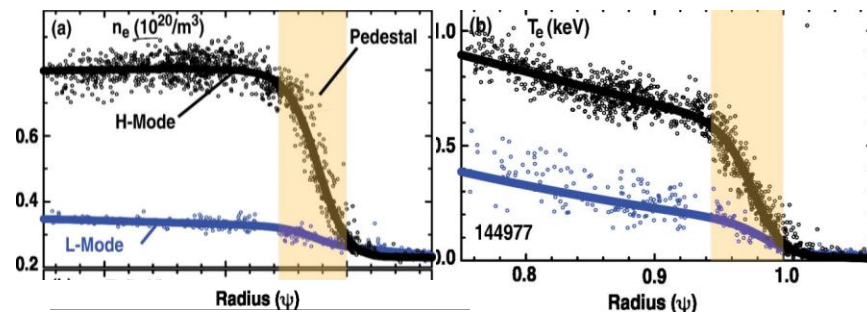


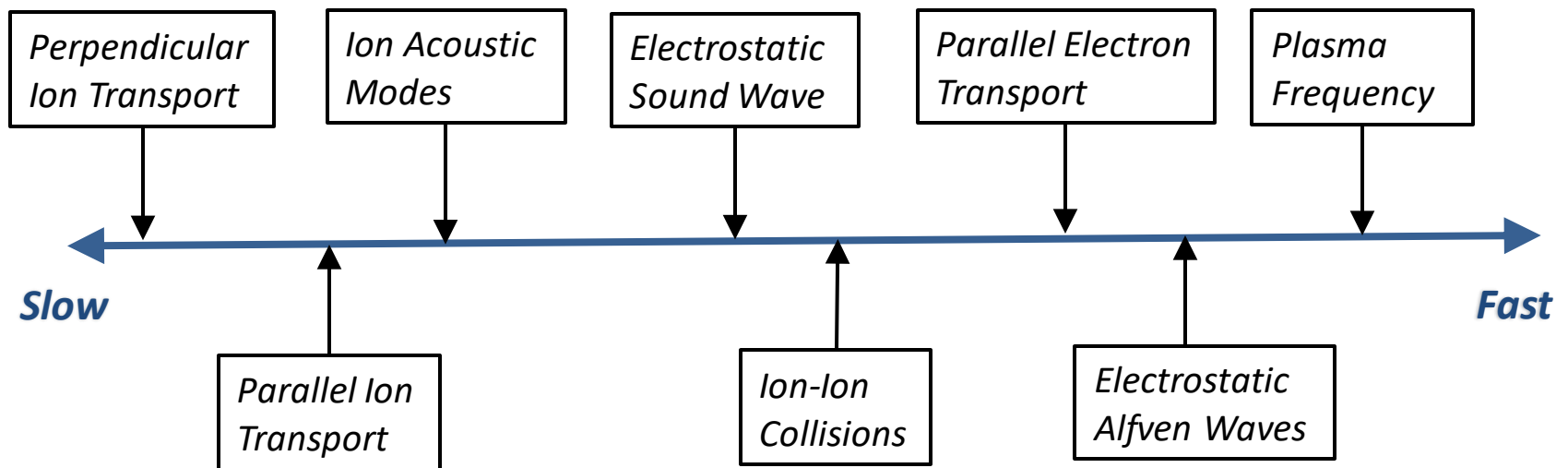
Image source:
www.iter.org



A. W. Leonard, Phys. Plasmas 21, 090501 (2014)

Time Scales and Time Integration

Tokamak edge plasma dynamics is characterized by a **large range of time scales**



Explicit time-integration constrained by *fastest time scale in the model*

- *Inefficient when resolving slow dynamics*

Implicit time-integration requires solution to *nonlinear system of equations*

- *Unconditional stability*
- *Pay for inverting terms we want to resolve?*

Which time scales do we want to resolve? (Usually, some of them)

COGENT: *High-Order Finite-Volume Gyrokinetic Code for Magnetized Plasma Dynamics*

Physics/Mathematical characteristics

*High dimensionality
(kinetic modelling)*

Numerical Conservation

*Complex geometry and anisotropy
(tokamak edge, Z-pinch)*

Multiple time scales

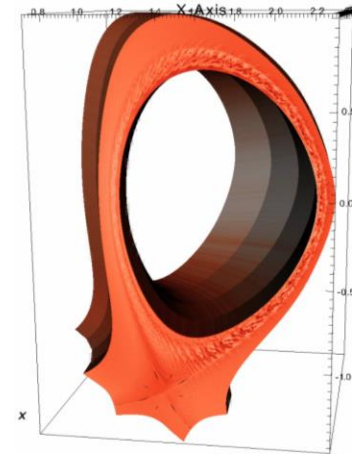
Algorithm choice

High-order spatial
discretization

Finite volume
discretization;
Conservative semi-implicit time
integration

Mapped, multiblock, field-aligned grids

Implicit-explicit (IMEX) time integration
(high-order additive Runge-Kutta methods)



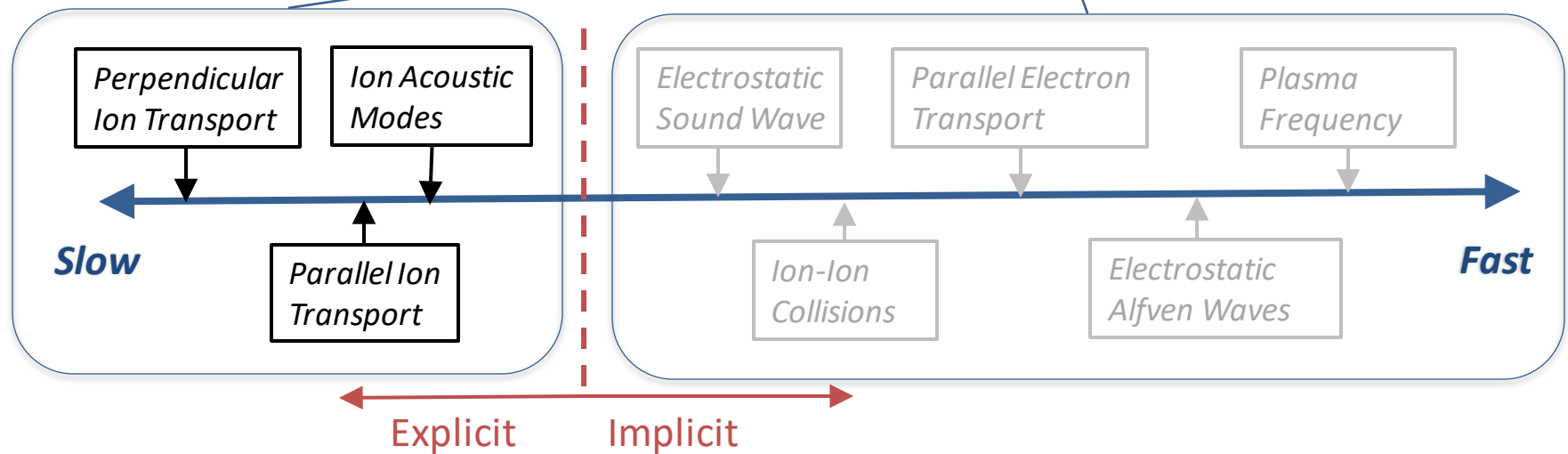
Implicit-Explicit (IMEX) Time Integration

Resolve scales of interest; Treat implicitly faster scales

ODE in time Resulting from spatial discretization of PDE $\frac{dy}{dt} = \mathcal{R}(y)$

IMEX time integration:
partition RHS

$$\mathcal{R}(y) = \mathcal{R}_{\text{nonstiff}}(y) + \mathcal{R}_{\text{stiff}}(y)$$

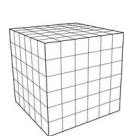


Time step constrained by
fastest explicit time scale

Flexible, user-specified partitioning of various physics terms depending on the time scale of interest

Governing Equations: Cross-Separatrix Transport Model with Self-Consistent Electric Fields

Phase-space collisional drift-kinetic model (4D/5D) – ion species



$$\frac{\partial (B_{\parallel\alpha}^* f_{\alpha})}{\partial t} + \nabla_{\mathbf{X}} \cdot (\dot{\mathbf{X}}_{\alpha} B_{\parallel\alpha}^* f_{\alpha}) + \frac{\partial}{\partial v_{\parallel}} (\dot{v}_{\parallel\alpha} B_{\parallel\alpha}^* f_{\alpha}) = \mathcal{C} [B_{\parallel\alpha}^* f_{\alpha}]$$

Fokker-Planck collision model

where

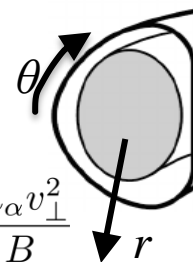
$$\dot{\mathbf{X}}_{\alpha} = \frac{1}{B_{\parallel\alpha}^*} \left[v_{\parallel} \mathbf{B}_{\alpha}^* + \frac{1}{Z_{\alpha} e} \mathbf{b} \times (Z_{\alpha} e \nabla \phi + \mu \nabla B) \right],$$

$$\dot{v}_{\parallel\alpha} = -\frac{1}{m_{\alpha} B_{\parallel\alpha}^*} \mathbf{B}_{\alpha}^* \cdot (Z_{\alpha} e \nabla \phi + \mu \nabla B)$$

Physical and velocity coordinates

$$\mathbf{X} \equiv \{r, \theta\}$$

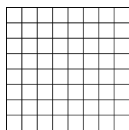
$$v_{\parallel}, \mu = \frac{1}{2} \frac{m_{\alpha} v_{\perp}^2}{B}$$



Configuration-space self-consistent, quasineutral model (2D/3D) – electrostatic potential

$$\frac{\partial}{\partial t} \left[\nabla_{\perp} \cdot \left(\frac{e^2 n_i}{m_i \Omega_i^2} \nabla_{\perp} \phi \right) \right] = \nabla_{\perp} \cdot \mathbf{j}_{i,\perp} + \nabla_{\parallel} \left[\sigma_{\parallel} \left(\frac{1}{en_i} \nabla_{\parallel} P_e - \nabla_{\parallel} \phi + \frac{0.71}{e} \nabla_{\parallel} T_e \right) \right]$$

$$- \nabla_{\perp} \cdot \left(\frac{c^2 m_i n_i \nu_{ex}}{B^2} \nabla_{\perp} \phi \right)$$



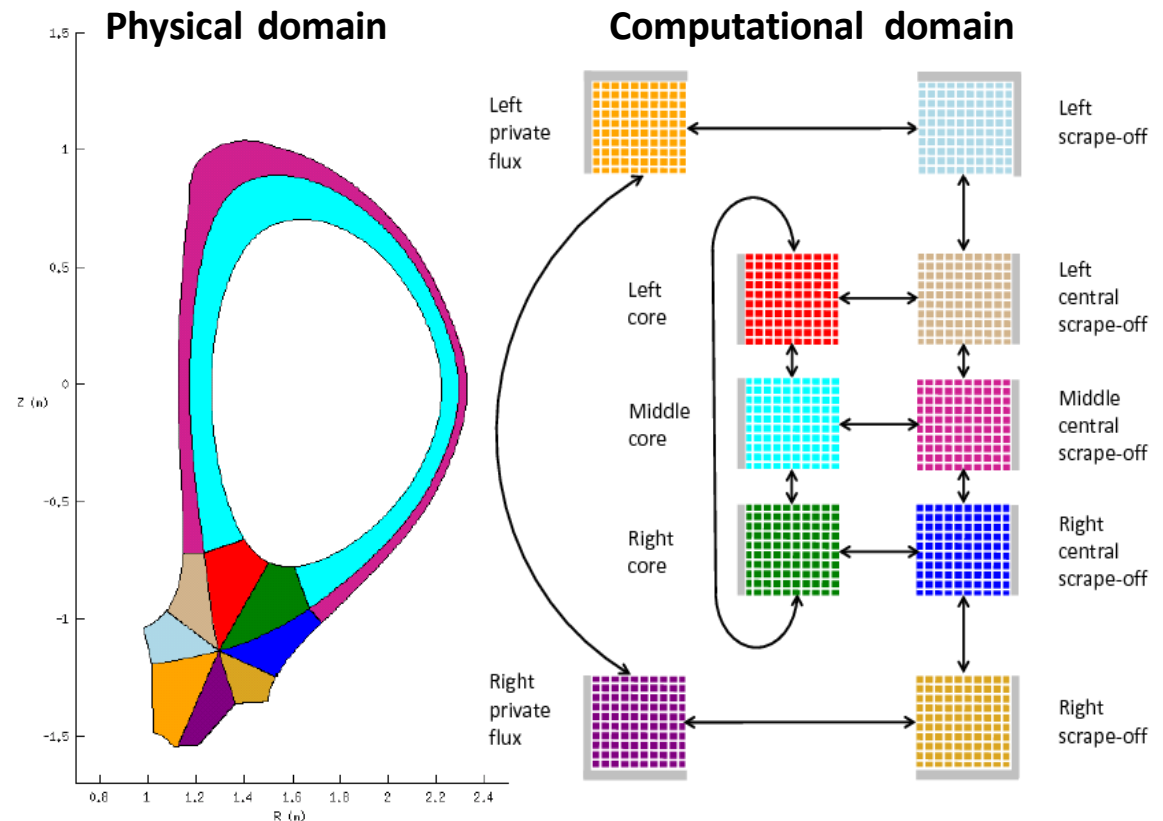
Solved on a mapped, multi-block mesh representing the tokamak edge



Reference: Dorf & Dorr, 2018, Contrib. Plasma Phys.

Spatial Discretization: Mapped Multiblock Grids

- Spatial discretization uses **Chombo**
- Domain decomposed into **multiple blocks**
- Each block mapped to a **Cartesian hypercube** with uniform grid
- High-order finite volume discretization requires extended **smooth block mappings**
- One of the coordinates is **aligned along the magnetic flux** lines (2D) or surfaces (3D)



Example: Ten-block grid for the DIII-D geometry

Reference: Dorr Et Al., 2018, J. Comput. Phys.

Semi-Discretized ODE and Stiff Terms

Semi-discrete ODE for the kinetic ions $\frac{d\mathbf{f}}{dt} = \mathcal{V}(\mathbf{f}, \Phi) + \mathcal{C}(\mathbf{f})$

Semi-discrete ODE for the electrostatic potential $\frac{d}{dt} [\mathcal{M}(\mathbf{f}) \Phi] = \mathcal{R}_\perp(\mathbf{f}, \Phi) + \mathcal{R}_\parallel(\mathbf{f}, \Phi)$ *ODE with nonlinear LHS operator*

$\downarrow \nabla_\perp \cdot \left(\frac{e^2 n_i}{m_i \Omega_i^2} \nabla_\perp \phi \right) \rightarrow \mathcal{M}(\mathbf{f}) \Phi$

$$\mathbf{f} = \begin{bmatrix} \vdots \\ B_{\parallel\alpha}^* f_\alpha \\ \vdots \end{bmatrix}$$

$$\Phi = \begin{bmatrix} \vdots \\ \phi \\ \vdots \end{bmatrix} \quad (\text{vectors of solution at grid points})$$

Partitioned system of ODEs for IMEX time integration

$$\frac{d}{dt} [\mathbb{M}(\mathbf{U})] = \mathcal{R}_{\text{nonstiff}}(\mathbf{U}) + \mathcal{R}_{\text{stiff}}(\mathbf{U})$$

where $\mathbf{U} \equiv \begin{bmatrix} \mathbf{f} \\ \Phi \end{bmatrix}$, $\mathbb{M} \equiv \begin{bmatrix} \mathcal{I} & 0 \\ 0 & \mathcal{M} \end{bmatrix}$, $\mathcal{R}_{\text{nonstiff}} \equiv \begin{bmatrix} \mathcal{V}(\mathbf{f}, \Phi) \\ \mathcal{R}_\perp(\mathbf{f}, \Phi) \end{bmatrix}$,

Fast timescales: kinetic collisions and parallel current divergence

$$\mathcal{R}_{\text{stiff}} \equiv \begin{bmatrix} \mathcal{C}(\mathbf{f}) \\ \mathcal{R}_\parallel(\mathbf{f}, \Phi) \end{bmatrix}$$

Additive Runge-Kutta (ARK) Time Integration

Modified for nonlinear LHS term

Time step: From t_n to $t_{n+1} = t_n + \Delta t$

Stage solutions

$$\mathbb{M}(\mathbf{U}^{(i)}) = \mathbb{M}(\mathbf{U}^n) + \Delta t \left[\sum_{j=1}^{i-1} a_{ij} \mathcal{R}_{\text{nonstiff}}(\mathbf{U}^{(j)}) + \sum_{j=1}^i \tilde{a}_{ij} \mathcal{R}_{\text{stiff}}(\mathbf{U}^{(j)}) \right], \quad i = 1, \dots, s$$

Step Completion

$$\mathbb{M}(\mathbf{U}^{n+1}) = \mathbb{M}(\mathbf{U}^n) + \Delta t \sum_{i=1}^s b_i \left[\mathcal{R}_{\text{nonstiff}}(\mathbf{U}^{(i)}) + \mathcal{R}_{\text{stiff}}(\mathbf{U}^{(i)}) \right]$$

Standard ARK methods if $\mathbb{M}(\mathbf{U}) = \mathbf{U}$

Note: “Explicit” stages and step completion **also require solution to nonlinear system of equations**

Butcher tableaux representation of time integrator

0	0	<i>Explicit RK</i>			+	0	0	<i>First-stage-explicit DIRK</i>		
c_2	a_{21}	0				\tilde{c}_2	\tilde{a}_{21}	γ		
\vdots	\vdots	\ddots	0			\vdots	\vdots	\ddots	γ	
c_s	a_{s1}	\cdots	$a_{s,s-1}$	0		\tilde{c}_s	\tilde{a}_{s1}	\cdots	$\tilde{a}_{s,s-1}$	γ
	b_1	\cdots	\cdots	b_s			b_1	\cdots	\cdots	b_s

ARK2c: 2nd order, 3-stage
(Giraldo, et al, 2013, SISC)

ARK3: 3rd order, 4-stage
(Kennedy & Carpenter, 2003, JCP)

ARK4: 4th order, 6-stage
(Kennedy & Carpenter, 2003, JCP)

Reference: Kennedy & Carpenter, 2003, J. Comput. Phys.

JFNK Solver for Nonlinear System

We need to solve a *nonlinear system of equations* at each time integration stage and at step completion

“Explicit” stages and step completion

$$\mathbb{M}(\mathbf{U}) = \mathbf{rhs}$$

Implicit stages

$$\alpha \mathbb{M}(\mathbf{U}) - \mathcal{R}_{\text{stiff}}(\mathbf{U}) = \mathbf{rhs}$$

$$\text{where } \alpha = 1 / (\tilde{a}_{ii} \Delta t)$$

Jacobian-free Newton-Krylov (JFNK) method :

(Initial guess is previous stage solution)

Newton update:

$$y_{k+1} = y_k - \mathcal{J}(y_k)^{-1} \mathcal{F}(y_k)$$

Preconditioned GMRES

$$\mathcal{J} \mathcal{P}^{-1} \mathcal{P} \Delta y = \mathcal{F}(y_k)$$

Action of the Jacobian on a vector approximated by *directional derivative*

$$\mathcal{J}(y_k) x = \left. \frac{d\mathcal{F}(y)}{dy} \right|_{y_k} x \approx \frac{1}{\epsilon} [\mathcal{F}(y_k + \epsilon x) - \mathcal{F}(y_k)]$$

Reference: Knoll & Keyes, 2004, *J. Comput. Phys.*

Operator-Split Multiphysics Preconditioner (1)

The **implicit RHS** comprises an **arbitrary number of terms**

$$\mathcal{R}_{\text{stiff}}(\mathbf{U}) = \sum_k \mathcal{F}_k(\mathbf{U})$$



Jacobian

$$\left[\alpha \mathbb{M}'(\mathbf{U}) - \sum_k \mathcal{F}'_k(\mathbf{U}) \right]$$



Approximation for Preconditioner

$$\left[\alpha \tilde{\mathbb{M}}'(\mathbf{U}) - \sum_k \tilde{\mathcal{F}}'_k(\mathbf{U}) \right]$$

$$\tilde{\mathbb{M}}' \approx \mathbb{M}', \tilde{\mathcal{F}}'_k \approx \mathcal{F}'_k$$

Operator-split wrapper over preconditioners for each individual physics term(s)

$$\left[\alpha \tilde{\mathbb{M}}'(\mathbf{U}) - \sum_k \tilde{\mathcal{F}}'_k(\mathbf{U}) \right] \mathbf{x} = \mathbf{b}$$



$$\Rightarrow \mathbf{x} = \prod_{k=N}^2 \left([\alpha \mathbb{M}' - \mathcal{F}'_k]^{-1} [\alpha \mathbb{M}'] \right) [\alpha \mathbb{M}' - \mathcal{F}'_1]^{-1} \mathbf{b}$$

- Operator-split approach **wraps multiple independent preconditioners for each term(s)** with fast time scales to precondition the complete implicit solve, *instead of a monolithic preconditioner*
- An **efficient preconditioning strategy** (matrix construction and solver) can be chosen specifically **for each implicit physics independent of other implicit terms**
- Applying (inverting) the preconditioner requires the **successive application of these individual preconditioners** on the solution vector

Operator-Split Multiphysics Preconditioner (2)

Implicit kinetic term: *Fokker-Planck-Rosenbluth collision term*

$$c[f_\alpha, f_\alpha] = \lambda_c \left(\frac{4\pi Z_\alpha^2 e^2}{m_\alpha} \right)^2 \nabla_{(v_\parallel, \mu)} \cdot \left[\vec{\gamma}_\alpha f_\alpha + \overleftarrow{\tau}_\alpha \nabla_{(v_\parallel, \mu)} f_\alpha \right]$$

where the advective and diffusive coefficients are given by

$$\vec{\gamma}_\alpha = \begin{bmatrix} \frac{\partial \varphi_\alpha}{\partial v_\parallel} & 2\mu \frac{m_\alpha}{B} \frac{\partial \varphi_\alpha}{\partial \mu} \end{bmatrix}, \quad \overleftarrow{\tau}_\alpha = \begin{bmatrix} -\frac{\partial^2 \varphi_\alpha}{\partial v_\parallel^2} & -2\mu \frac{m_\alpha}{B} \frac{\partial^2 \varphi_\alpha}{\partial v_\parallel \partial \mu} \\ -2\mu \frac{m_\alpha}{B} \frac{\partial^2 \varphi_\alpha}{\partial v_\parallel \partial \mu} & -2\mu \left(\frac{m_\alpha}{B} \right)^2 \left\{ 2\mu \frac{\partial^2 \varphi_\alpha}{\partial \mu^2} + \frac{\partial \varphi_\alpha}{\partial \mu} \right\} \end{bmatrix}$$

$\mathcal{C}(\tilde{f})$ 5th order upwind (advection)
4th order central (diffusion)

$\bar{\mathcal{C}}(\tilde{f})$ 1st order upwind (advective)
2nd order central (diffusion)

Results in a **9-banded matrix**;
inverted with **Gauss-Seidel**

Implicit fluid terms: *Elliptic LHS Op and parallel current divergence*

$$\nabla_\perp \cdot \left(\frac{e^2 n_i}{m_i \Omega_i^2} \nabla_\perp \phi \right)$$

$$\nabla_\parallel \left[\sigma_\parallel \left(\frac{1}{en_i} T_e \nabla_\parallel n_i - \nabla_\parallel \phi \right) \right]$$

Discretized with 4th order mapped finite volume method

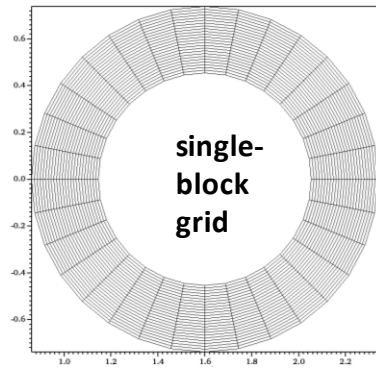
Jacobian approximation constructed with 2nd order mapped finite-difference discretization



Solved with the **Algebraic Multigrid (AMG) method** implemented in the *hypra* library

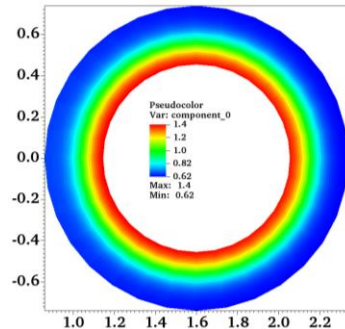
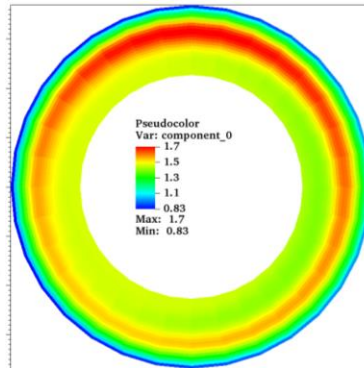
Test Cases: Tokamak Edge Simulations

Kinetic Ion Species with Fokker-Plank Collisions and Fluid Potential Model



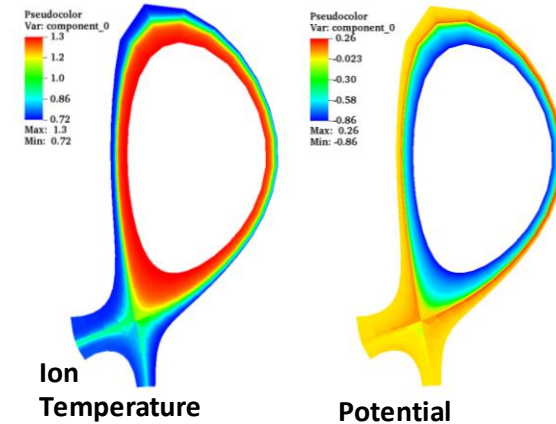
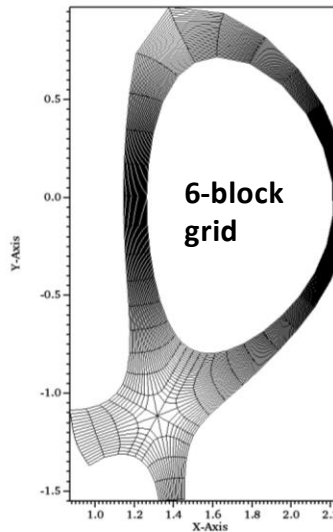
Neoclassical thermal relaxation in **annular geometry**

Ion Temperature @ 4ms



Initial Ion Temperature

Plasma equilibration under H-mode parameters in **DIII-D tokamak**



Solution at $t = 2.8ms$

Reference: Dorf & Dorr, 2018, Contrib. Plasma Phys.

Weakly collisional simulations

Kinetic equation: *completely explicit*

Fluid potential equation: **parallel current**

divergence implicit; perpendicular terms explicit

Strongly collisional simulations

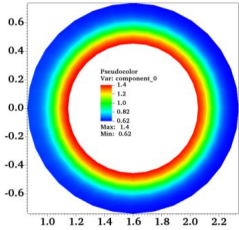
Kinetic equation: **Collisions implicit**; Vlasov explicit

Fluid potential equation: **parallel current**

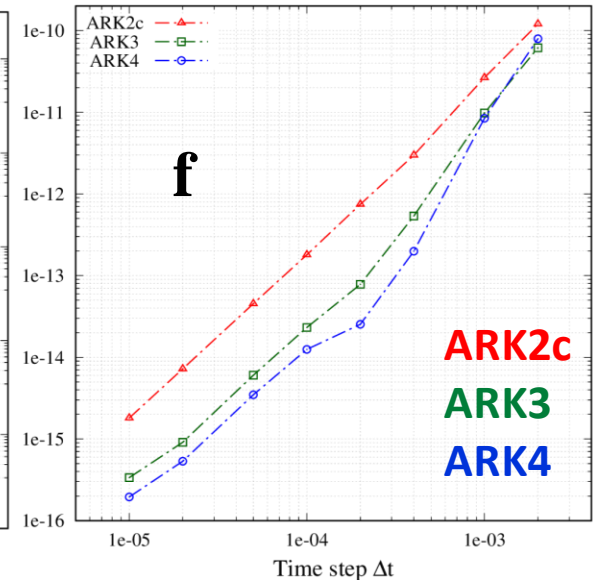
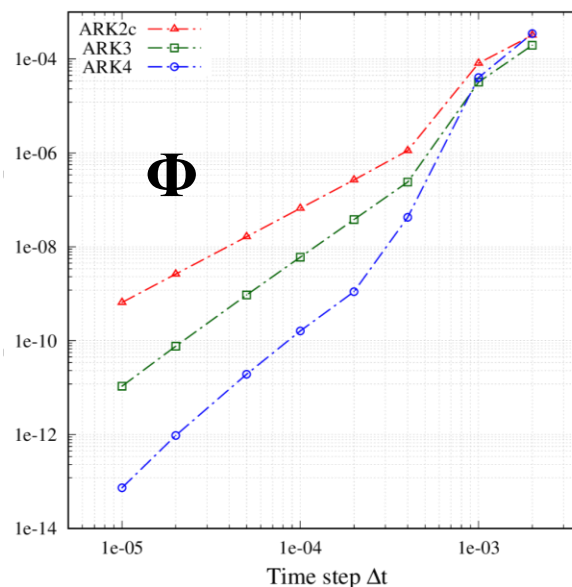
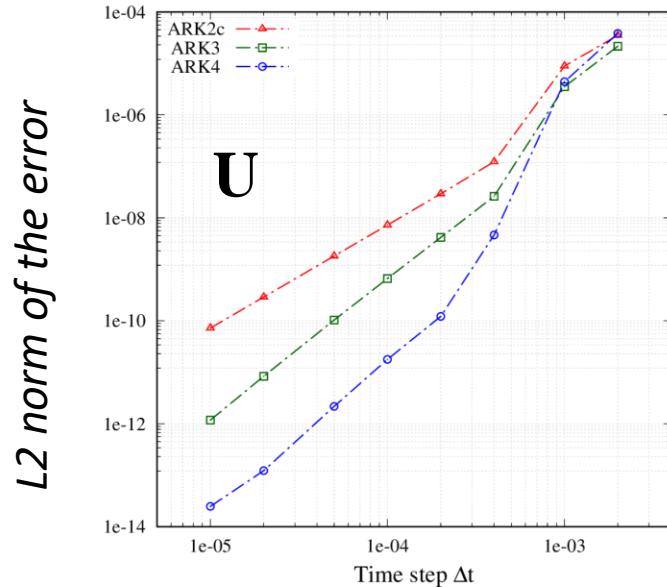
divergence implicit; perpendicular terms explicit

Test Case: Neoclassical Thermal Relaxation

Weakly-collisional



- **Electrostatic potential (Φ)** converges at the theoretical orders (*semi-implicit in time, with **nonlinear LHS operator***)
- **Distribution function (f)** converges at **$\sim 2nd$ order (?)** (*completely explicit in time*)

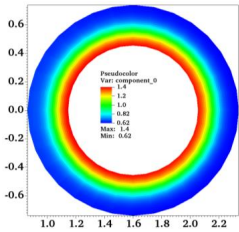


Final time $t_f = 0.002$ (normalized units); **Timescales:** ~ 0.1 (Vlasov), ~ 5 (Collisions)

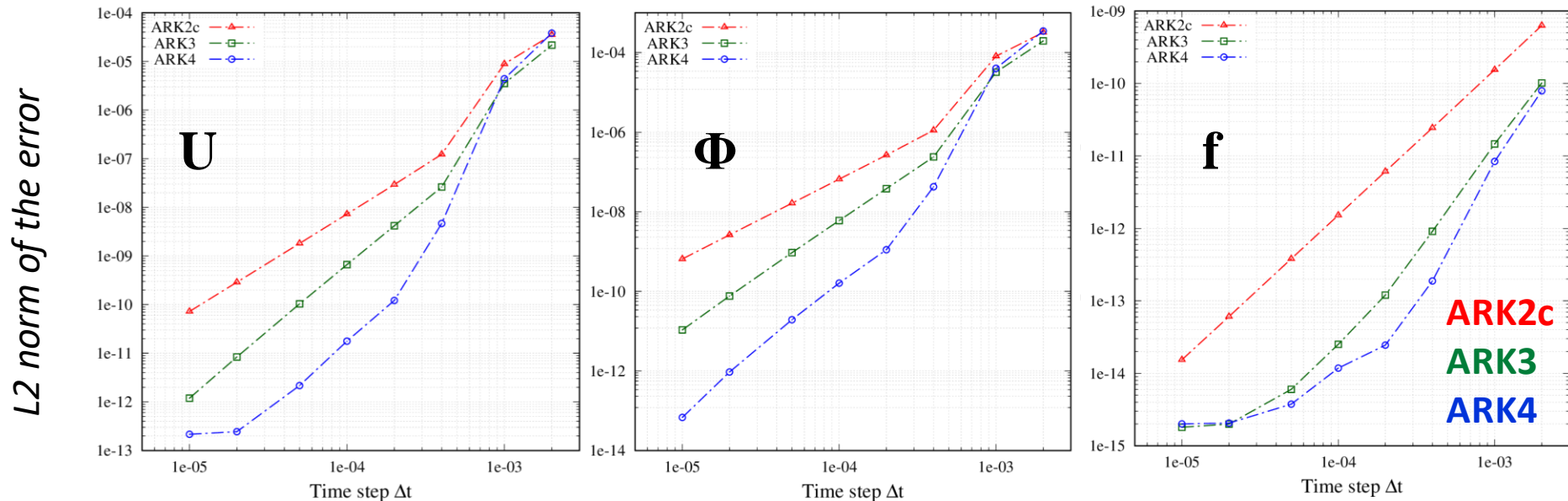
Reference solution generated with ARK4 at $\Delta t_{ref} = 0.05 \Delta t_{min}$ in convergence study

Test Case: Neoclassical Thermal Relaxation

Strongly-collisional



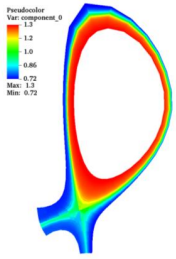
- **Electrostatic potential (Φ)** converges at the theoretical orders (*semi-implicit in time, with **nonlinear LHS operator***)
- **Distribution function (f)** converges **at theoretical order** for ARK2c and ARK3 (*implicit collisions, explicit Vlasov in time*)



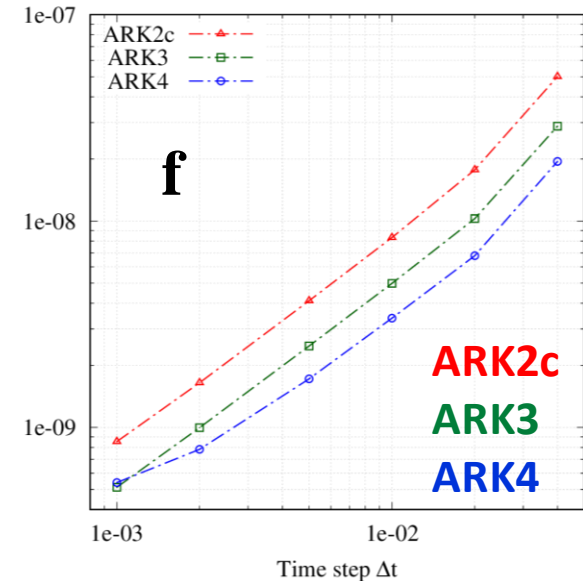
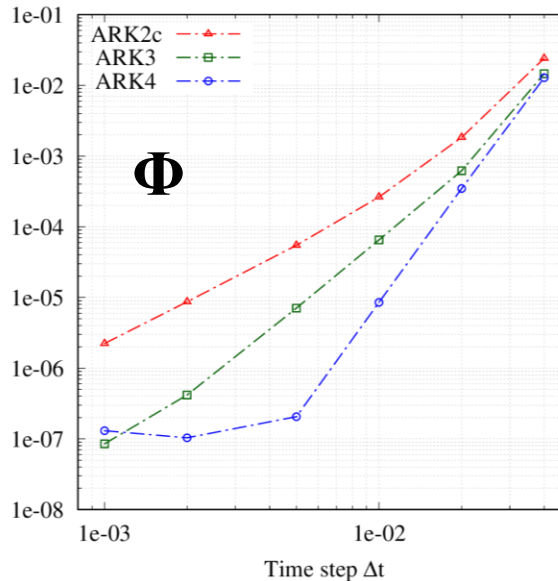
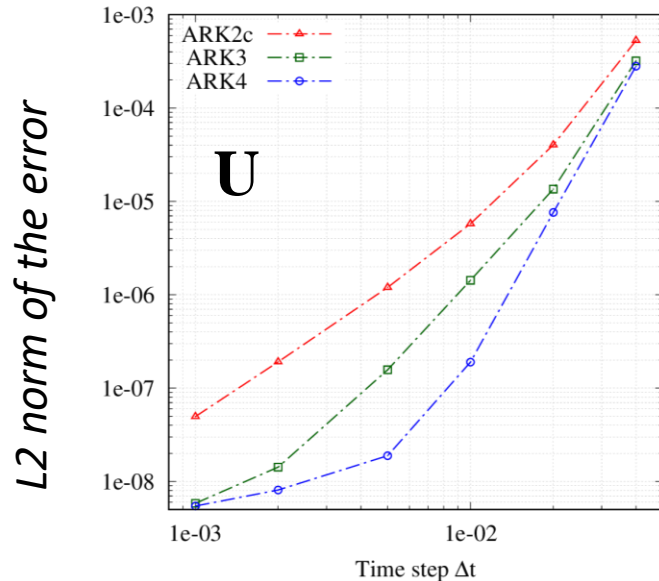
Final time $t_f = 0.002$ (normalized units); **Timescales:** ~ 0.1 (Vlasov), $\sim 5e-3$ (Collisions)
Reference solution generated with ARK4 at $\Delta t_{ref} = 0.05 \Delta t_{min}$ in convergence study

Test Case: DIII-D Tokamak H-Mode Simulation

Weakly-collisional



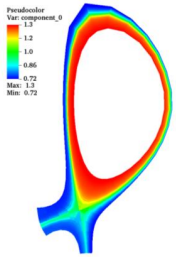
- **Electrostatic potential (Φ)** converges at the theoretical orders (*semi-implicit in time, with **nonlinear LHS operator***)
- **Distribution function (f)** converges at **$\sim 1st$ order** (*completely explicit in time*)



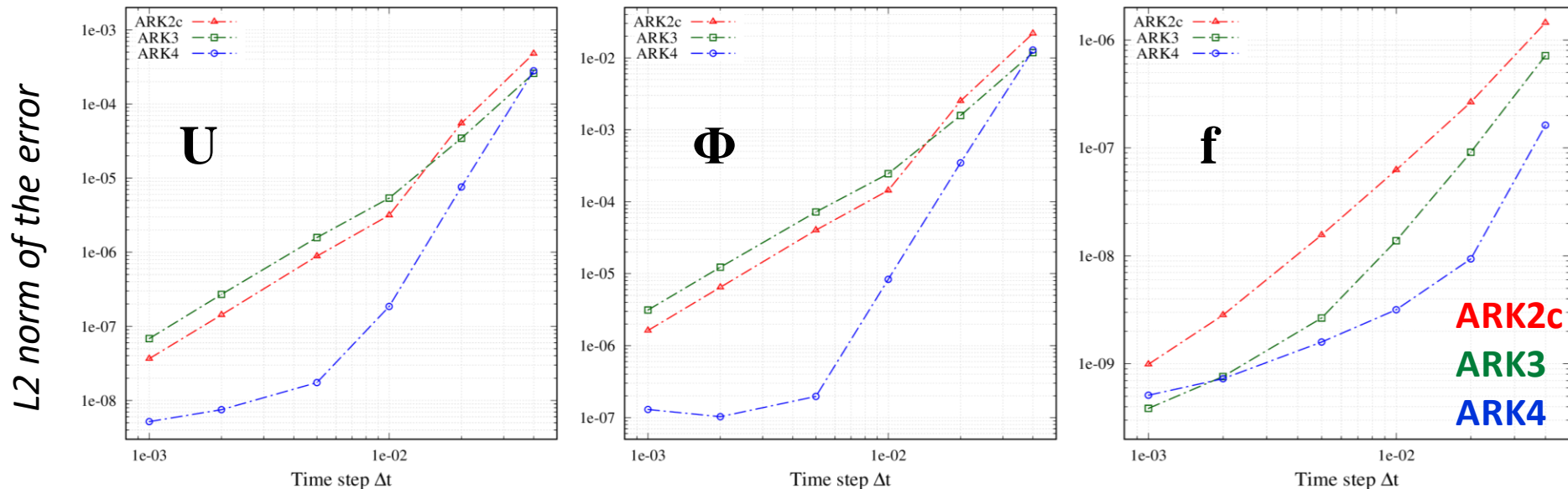
Final time $t_f = 0.040$ (normalized units); **Timescales:** $\sim 7e-2$ (Vlasov), ~ 0.7 (Collisions)
Reference solution generated with ARK4 at $\Delta t_{ref} = 0.05 \Delta t_{min}$ in convergence study

Test Case: DIII-D Tokamak H-Mode Simulation

Strongly-collisional



- **Electrostatic potential (Φ)**: ARK2c and ARK4 converge as expected; ARK3 converges at **2nd order** (*semi-implicit in time, with **nonlinear LHS operator***)
- **Distribution function (f)**: ARK2c and ARK3 converge as expected; ARK4 converges at **4th order** initially, then **$\sim 1st$ order** (*completely explicit in time*)



Final time $t_f = 0.040$ (normalized units); **Timescales**: $\sim 7e-2$ (Vlasov), $\sim 8e-3$ (Collisions)

Reference solution generated with ARK4 at $\Delta t_{ref} = 0.05 \Delta t_{min}$ in convergence study

Summary

- **COGENT** is a high-order mapped multiblock code for tokamak-edge plasma dynamics
 - **Open source:** <https://github.com/LLNL/COGENT>
- We have implemented a **flexible implicit-explicit (IMEX) time integration framework** that allows user-specified partitioning of the various terms into the implicit and explicit sides.
 - Modified the standard Additive Runge-Kutta methods to allow for a *nonlinear left-hand-side operator*
- **Operator-split preconditioning** acts as a wrapper for tailored preconditioners for each implicit term to precondition the complete implicit solve
- We are testing **time convergence** for simulations on **mapped multiblock grids**
 - Obtained **theoretical convergence** in some cases; currently investigating cause of sub-optimal convergence.



CASC

Center for Applied
Scientific Computing

**Thank you.
Questions?**

Disclaimer

This document was prepared as an account of work sponsored by an agency of the United States government. Neither the United States government nor Lawrence Livermore National Security, LLC, nor any of their employees makes any warranty, expressed or implied, or assumes any legal liability or responsibility for the accuracy, completeness, or usefulness of any information, apparatus, product, or process disclosed, or represents that its use would not infringe privately owned rights. Reference herein to any specific commercial product, process, or service by trade name, trademark, manufacturer, or otherwise does not necessarily constitute or imply its endorsement, recommendation, or favoring by the United States government or Lawrence Livermore National Security, LLC. The views and opinions of authors expressed herein do not necessarily state or reflect those of the United States government or Lawrence Livermore National Security, LLC, and shall not be used for advertising or product endorsement purposes.

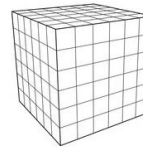


“Multiple-Dimensioned” Governing Equations

COGENT can evolve an arbitrary combination of PDEs of *varying dimensionality* (kinetic and fluid) with a high-order, consistent discretization

Phase-space kinetic equations (4D/5D) – ions, electron

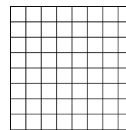
$$\frac{\partial f}{\partial t} + \nabla_{\mathbf{x}} \cdot (\dot{\mathbf{x}} [f, \phi] f) + \frac{\partial}{\partial v_{\parallel}} (\dot{v}_{\parallel} [f, \phi] f) = C [f]$$



Configuration space fluid/field equations (2D/3D)

– ions, electron, vorticity, neutrals

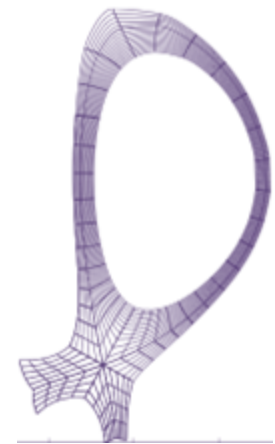
$$\frac{\partial \phi}{\partial t} + \nabla_{\mathbf{x}} \cdot \mathbf{F} (f, \phi) = \nabla_{\mathbf{x}} (\nabla_{\mathbf{x}} \cdot \mathbf{G} (f, \phi))$$



+ any closure equations (e.g., gyro-Poisson equation for electrostatic potential or any other equation to complete the system)

Number of kinetic and fluid equations is flexible and user-specified, including capability for kinetic-only or fluid-only simulations

Solved on a mapped, multi-block mesh representing the tokamak edge



COGENT is part of the Edge Simulation Laboratory collaboration between US DOE ASCR and FES



Math (ASCR)



L. Ricketson
M. Dorr
D. Ghosh
P. Tranquilli



D. Martin
P. Colella
P. Schwartz

Physics (FES)



M. Dorf
V. Geyko
J. Angus

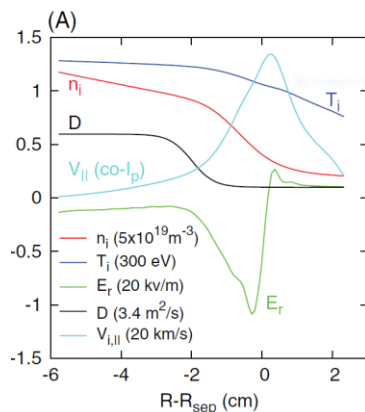


P. Snyder
J. Candy
E. Belli

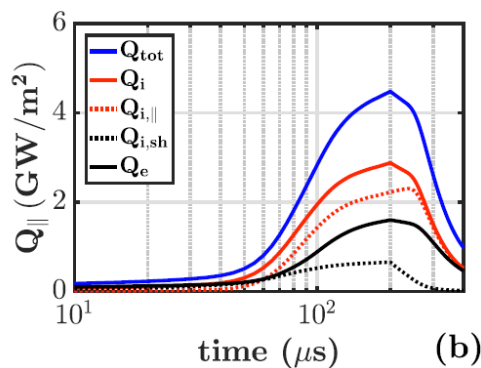


S. Krasheninnikov

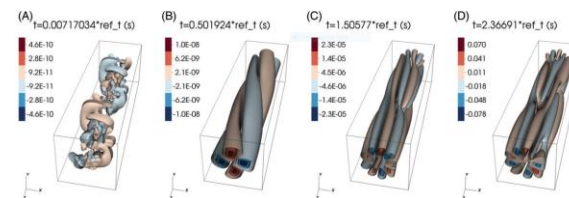
Cross separatrix transport (Dorf et al., Contrib. Plasma Phys., 58, 434-444, 2018)



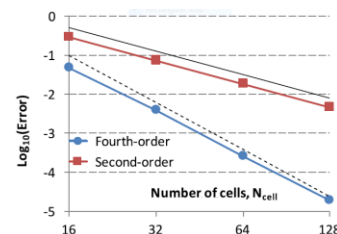
ELM heat pulse (Joseph et al., Nucl. Mater. Energy, 19, 330-334, 2019)



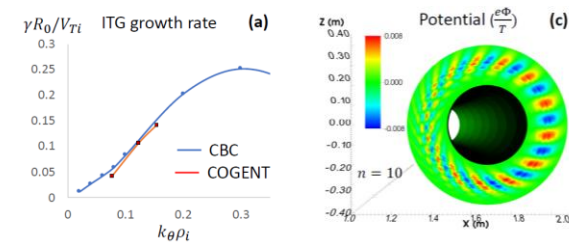
Kinetic drift-wave instability (Lee et al., Contrib. Plasma Phys., 58, 445-450, 2018)



High-order drift wave modeling (Dorf et al., J. Comput. Phys., 373, 446-545, 2018)



5-D full-f gyrokinetic code COGENT (Dorf et al., Contrib. Plasma Phys., 2020)

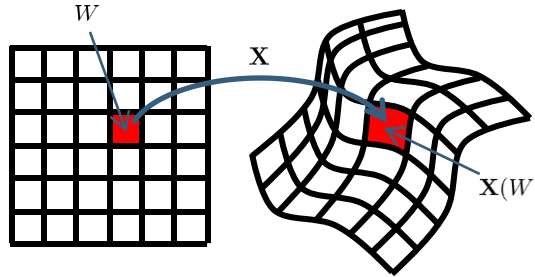


4th Order Mapped Finite-Volume Discretization

Computational coordinates:

Spatial domain discretized by rectangular control volumes

$$V_i = \prod_{d=1}^D \left[i_d - \frac{h}{2}, i_d + \frac{h}{2} \right]$$



$$\mathbf{X} \equiv \mathbf{X}(\xi), \quad \mathbf{X} : [0, 1]^D \rightarrow \Omega \subset \mathbb{R}^D$$

Mapped coordinates:

Mapping from abstract Cartesian coordinates into physical space

$$\mathbf{X} = \mathbf{X}(\xi), \quad \mathbf{X} : [0, 1]^D \rightarrow \mathbb{R}^D$$

Fourth-order flux divergence average from fourth-order cell face averages

$$\int_{\mathbf{X}(V_i)} \nabla_{\mathbf{X}} \cdot \mathbf{F} d\mathbf{x} = \sum_{\pm=+,-} \sum_{d=1}^D \pm \int_{A_d^{\pm}} (\mathbf{N}^T \mathbf{F})_d d\mathbf{A}_{\xi} = h^{D-1} \sum_{\pm=+,-} \sum_{d=1}^D \pm F_{i \pm \frac{1}{2} \mathbf{e}^d}^d + O(h^4)$$

where

$$(\mathbf{N}^T)_{p,q} = \det \left(\mathbf{R}_p \left(\frac{\partial \mathbf{X}}{\partial \xi}, \mathbf{e}^q \right) \right) \quad \mathbf{R}_p(\mathbf{A}, \mathbf{v}) : \text{replace } p\text{-th row of } \mathbf{A} \text{ with } \mathbf{v}$$

$$F_{i \pm \frac{1}{2} \mathbf{e}^d}^d = \sum_{s=1}^D \langle N_d^s \rangle_{i \pm \frac{1}{2} \mathbf{e}^d} \langle F^s \rangle_{i \pm \frac{1}{2} \mathbf{e}^d} + \frac{h^2}{12} \sum_{s=1}^D \left(\mathbf{G}_0^{\perp,d} \left(\langle N_d^s \rangle_{i \pm \frac{1}{2} \mathbf{e}^d} \right) \right) \cdot \left(\mathbf{G}_0^{\perp,d} \left(\langle F^s \rangle_{i \pm \frac{1}{2} \mathbf{e}^d} \right) \right)$$

$$\mathbf{G}_0^{\perp,d} = \text{second-order accurate centered difference of } \nabla_{\xi} - \mathbf{e}^d \frac{\partial}{\partial \xi_d} \quad \langle q \rangle_{i \pm \frac{1}{2} \mathbf{e}^d} \equiv \frac{1}{h^{D-1}} \int_{A_d} q(\xi) d\mathbf{A}_{\xi} + O(h^4)$$